In *Candida albicans*, phosphorylation of Exo84 by Cdk1-Hgc1 is necessary for efficient hyphal extension

David Caballero-Lima and Peter E. Sudbery
Department of Molecular Biology and Biotechnology, University of Sheffield, Western Bank, Sheffield S10 2TN, United Kingdom

ABSTRACT **The exocyst, a conserved multiprotein complex, tethers secretory vesicles before fusion with the plasma membrane; thus it is essential for cell surface expansion. In both *Saccharomyces cerevisiae* and mammalian cells, cell surface expansion is halted during mitosis. In *S. cerevisiae*, phosphorylation of the exocyst component Exo84 by Cdk1-Clb2 during mitosis causes the exocyst to disassemble. Here we show that the hyphae of the human fungal pathogen *Candida albicans* continue to extend throughout the whole of mitosis. We show that *Ca*Exo84 is phosphorylated by Cdk1, which is necessary for efficient hyphal extension. This action of Cdk1 depends on the hyphal-specific cyclin Hgc1, the homologue of G1 cyclins in budding yeast. Phosphorylation of *Ca*Exo84 does not alter its localization but does alter its affinity for phosphatidylserine, allowing it to recycle at the plasma membrane. The different action of Cdk1 on *Ca*Exo84 and *Sc*Exo84 is consistent with the different locations of the Cdk1 target sites in the two proteins. Thus this conserved component of polarized growth has evolved so that its phosphoregulation mediates the dramatically different patterns of growth shown by these two organisms.**

Monitoring Editor
Gero Steinberg
University of Exeter

Received: Nov 22, 2013
Revised: Jan 9, 2014
Accepted: Jan 29, 2014

INTRODUCTION

Candida albicans can grow in budding yeast both pseudohyphal and true hyphal forms (Sudbery *et al.*, 2004). This morphological plasticity is essential for virulence of this major human fungal pathogen. In the hyphal state, growth is highly polarized to the tip (Soll *et al.*, 1985). Such polarized growth requires a constant supply of secretory vesicles that fuse with the plasma membrane at the tip (Sudbery, 2011; Caballero-Lima *et al.*, 2013). These vesicles are necessary for cell surface expansion, as they supply the additional membrane necessary for expansion of the plasma membrane. Vesicles also deliver the means to synthesize new cell wall, such as integral membrane glucan synthases, which manufacture β1,3-glucan and β1,6-glucan, chitin synthases, cell wall–remodeling enzymes, and the mannosylated proteins that form the outer layer of the cell wall (Klis *et al.*, 2006). Studies in the model yeast *Saccharomyces cerevisiae* showed that before fusion, secretory vesicles must be tethered to the plasma membrane by an evolutionarily conserved, multiprotein complex called the exocyst. This complex consists of eight subunits: Sec3, Sec5, Sec6, Sec8, Sec10, Sec15, Exo70, and Exo84 (Terbush and Novick, 1995; Terbush *et al.*, 1996; Brennwald and Rossi, 2007; He and Guo, 2009; Heider and Munson, 2012). In *S. cerevisiae* these proteins localize to sites of polarized growth such as small buds and the site of septum formation. Sec3, as well as part of the Exo70 pool, is believed to localize independently of the cytoskeleton (Finger *et al.*, 1998; Boyd *et al.*, 2004). Exo70 is an effector of and interacts with the Rho-type GTPases Rho3 and Cdc42, and Sec3 interacts with Rho1 (Adamo *et al.*, 1999; Guo *et al.*, 2001; Zhang *et al.*, 2001; Roumanie *et al.*, 2005; He *et al.*, 2007b; Wu *et al.*, 2010). Both Exo70 and Sec3 interact with phosphoinositol 4,5-phosphate (He *et al.*, 2007a; Zhang *et al.*, 2008). The remaining exocyst components are believed to arrive on incoming vesicles (Boyd *et al.*, 2004).

This article was published online ahead of print in MBoC in Press (http://www.molbiolcell.org/cgi/doi/10.1091/mbc.E13-11-0688) on February 5, 2014.

Address correspondence to: Peter E. Sudbery (P.Sudbery@shef.ac.uk).

D.C.-L. conceived and designed the study with input from P.E.S. D.C.-L. performed all the experiments, except the live-cell movies, which were carried out by P.E.S. P.E.S and D.C.-L. interpreted the data. P.E.S. wrote the manuscript with input from D.C.-L.

The authors declare they have no conflict of interest

Abbreviations used: H, hyphae; PA, phosphotydic; PH, pseudohyphae; λPP, λ-phosphatase; PS, phosphoinositol serine; α-pS Cdk, monoclonal antibody to phosphorylated serine in the context of the full Cdk1 target motif; WT, wild type; Y, yeast.

In *C. albicans*, exocyst subunits localize to a surface crescent at the hyphal tip (Jones and Sudbery, 2010). In contrast, vesicle-associated proteins such as Sec4, Sec2, and Mlc1 localize to a subapical spot that is clearly distinct from the surface crescent of the exocyst and is reminiscent of the Spitzenkörper long known to drive the polarized growth of other filamentous fungi (Crampin *et al.*, 2005; Bishop *et al.*, 2010; Jones and Sudbery, 2010). These different localization patterns suggest that at least during the polarized growth of hyphae, the exocyst is already present on the plasma membrane to tether the vesicles as they arrive. Such a notion is supported by fluorescence recovery after photobleaching (FRAP) and fluorescence loss in photobleaching (FLIP) experiments, which show that Sec2, Sec4, and Mlc1 are much more dynamic than exocyst components. Furthermore, disruption of the actin cytoskeleton leads to immediate dispersal of Sec4 from the Spitzenkörper, whereas exocyst components disperse more slowly from the surface crescent (Jones and Sudbery, 2010).

As well as controlling progress through the cell cycle, it is becoming increasingly apparent that the cyclin-dependent kinase Cdk1 (Cdc28) controls cell growth in *S. cerevisiae* (McCusker *et al.*, 2007; Goranov and Amon, 2010). In *C. albicans* the cyclin Hgc1 is specifically induced during hyphal growth and is necessary for normal hyphal morphology and growth (Zheng *et al.*, 2004). Hgc1 is the homologue of the Cln1/2 G1 cyclin pair of *S. cerevisiae*. Cells lacking Hgc1 are unable to maintain hyphal growth. When induced to form hyphae, such cells evaginate a normal germ tube, but this quickly swells, especially after the formation of the first septin ring. A number of targets for Cdk1-Hgc1 have been elucidated, such as the Cdc42 GAP Rga2, Sec2, the septin Cdc11, and the transcription factor Efg1 (Sinha *et al.*, 2007; Zheng *et al.*, 2007; Wang *et al.*, 2009; Bishop *et al.*, 2010). G2 cyclins in *C. albicans* are represented by Clb2, the orthologue of *S. cerevisiae* Clb2, and Clb4, the orthologue of *S. cerevisiae* Clb4. Clb2 is essential; depletion of Clb2 using the *MET3*-regulated promoter results in cell cycle arrest with highly elongated buds, whereas Δ*Clb4* cells are viable but show constitutive pseudohyphal growth (Bensen *et al.*, 2005).

In *S. cerevisiae* it was recently shown that phosphorylation of the exocyst subunit Exo84 by Cdk1-Clb2 causes cell growth to cease just before the metaphase-to-anaphase transition (Luo *et al.*, 2013). Exo84 plays a key role in the assembly of the exocyst. Its phosphorylation by Cdk1-Clb2 causes the exocyst complex to disassemble, blocking exocytosis and cell surface expansion. *Sc*Exo84 and *Ca*Exo84 show similar domain organization consisting of a coil-coiled Vps51 domain that in Vps51 is required for formation of the VFT docking complex mediating the fusion of late endosomes with the Golgi (Siniossoglou and Pelham, 2002), a central pleckstrin homology (PH) domain, and a C-terminal, rod-like domain composed of multiple α-helices that is responsible for the interaction with other members of the exocyst complex (Figure 1A). Luo *et al.* studied the effects of Clb2-Cdk1 phosphorylation of ScExo84 at two full Cdk1 consensus target sites (S/T.P.X.R/K) and three minimal target sites (S/T.P; Luo *et al.*, 2013). In view of the observation that phosphorylation of *Sc*Exo84 disrupts interaction with other exocyst subunits, it is significant that one of the full consensus sites in *Sc*Exo84 is located within the C-terminal interaction domain (S716). Of interest, there is no corresponding site in the C-terminal domain of *Ca*Exo84 (Figure 1, A and B). However, *Ca*Exo84 contains a full site within the PH domain (S384), which is absent in *Sc*Exo84 (Figure 1, A and B). Two additional full sites are located in *Ca*Exo84 at S256 and T488, which a Clustal alignment suggests may correspond to S291 and T496, respectively, in *Sc*Exo84 (Figure 1B). Modeling of *Ca*Exo84 shows that these sites are located on either side of the PH domain in the folded protein (Figure 1A).

Although cessation of cell growth during mitosis is a common feature among eukaryotic cells, we show here that *C. albicans* hyphae continue to grow throughout mitosis and cytokinesis. Moreover, localization of both the Spitzenkörper and the exocyst is unaltered throughout mitosis. However, we show that *Ca*Exo84 is phosphorylated by *Ca*Cdk1 in a hyphal-specific manner and that this phosphorylation is dependent on the hyphal-specific Hgc1 cyclin rather than a G2 cyclin. Moreover, in direct contrast to budding yeast, this phosphorylation of Exo84 is essential for rapid polarized growth of hyphae and normal hyphal morphology. Our study suggests that a role of phosphorylation is to dissociate Exo84 from the plasma membrane by lowering its affinity for phosphatidylserine.

RESULTS

C. albicans hyphae continue to grow throughout mitosis and cytokinetic ring contraction

To investigate whether *C. albicans* hyphae continue to extend throughout mitosis, we constructed strains in which the nucleolar protein Nop1 was fused to yellow fluorescent protein (YFP) to track the nucleus. In addition, we also fused either Mlc1 or Exo70 to YFP. Initially, we followed hyphal growth throughout two complete cells cycles in the strain expressing Nop1-YFP and Mlc1-YFP after hyphae were induced from stationary-phase, unbudded yeast cells. We recorded images at 60-s intervals (Supplemental Movie S1). As visualized by Nop1-YFP, the nucleus migrates out of the mother cell and divides within the germ tube, as reported previously (Sudbery, 2001). This is followed 20 min after anaphase by contraction of the cytokinetic ring visualized by Mlc1-YFP. A second anaphase occurs after 30 min, which in turn is followed by cytokinetic ring contraction 20 min later. Throughout the whole of these two cycles the hyphae extend at a constant rate of 0.33 μm/min (Supplemental Figure S1A). Close examination around the time of the two mitoses and the two contractions of the cytokinetic ring showed that hypha growth continued to extend during these events at a rate consistent with the long-term average rate of hyphal extension (Supplemental Figure S1, B and C).

It may be argued that the cessation of growth occurs on a shorter time scale than the 60-s intervals between frames in Supplemental Movie S1. We therefore investigated the growth of cells over shorter time scales. Moreover, it was of interest to visualize the Spitzenkörper, as this is a sensitive indicator of polarized growth of fungal hyphae, and the exocyst to discover whether it is dispersed as it is in *S. cerevisiae* during metaphase. We therefore recorded images over 10-s intervals throughout mitosis for the Nop1-YFP Mlc1-YFP strain and 20-s intervals for the Nop1-Exo70 strain. These experiments were complicated by the extreme sensitivity of mitosis to the excitation light; for this reason the frame rate was increased to 20 s for the Nop1-YFP Exo70 YFP strain. The full movies are Supplemental Movies S2 and S3 for Mlc1-YFP Nop1-YFP and Nop1-YFP Exo70-YFP, respectively. Consecutive frames spanning a mitosis are shown in Figure 2 for Mlc1-YFP Nop1-YFP and in Supplemental Figure S2 for Nop1-YFP Exo70-YFP. Of interest, in the Nop1-YFP Mlc1-YFP strain a pair of satellite spots appeared on either side of the nucleus just before anaphase, which may represent recruitment of myosin to the spindle pole body during metaphase. Evidence for a myosin role in the mitotic spindle has recently been reviewed (Sandquist *et al.*, 2011). Figure 2A shows that growth continued throughout mitosis, so that the tip extended by 0.8 μm in the 140-s of the movie shown in Figure 2A, consistent with the long-term average growth rate of

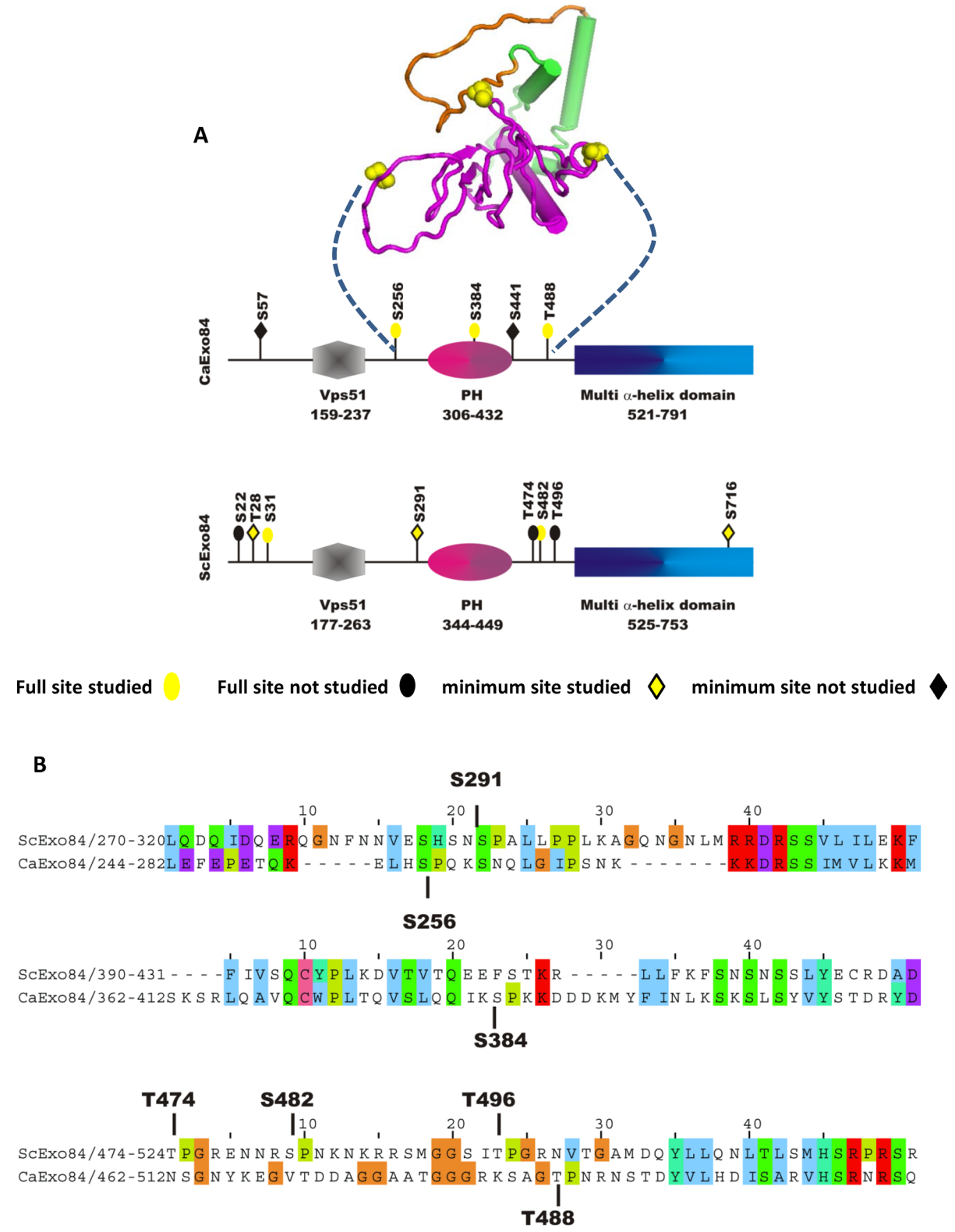

FIGURE 1: Domain organization and Cdk1 target sites of *Sc*Exo84 and *Ca*Exo84. (A) Domain organization and Cdk1 target sites. The VPS51 domain was identified in both CaExo84 and *ScExo84* using the Pfam database (Punta *et al.*, 2012). The PH domain and the C-terminal interaction domain were identified by threading as described in *Materials and Methods*. Studied sites refer to this article for *Ca*Exo84 and Luo *et al.* (2013) for *Sc*Exo84. The folding structure of the PH domain predicted by threading is shown in purple. Phosphorylation of potential Cdk1 target sites is shown by the yellow spheres. S284 lies within a protruding loop of the PH domain, and S256 and T488 are located at the boundaries of the PH domain. (B) Clustal alignments of sequences surrounding full Cdk1 sites in *Ca*Exo84. Color code follows standard Clustal X code: amino acids with similar properties are coded with the same color; the depth of the color denotes the degree of similarity, so that identical residues have the deepest color.

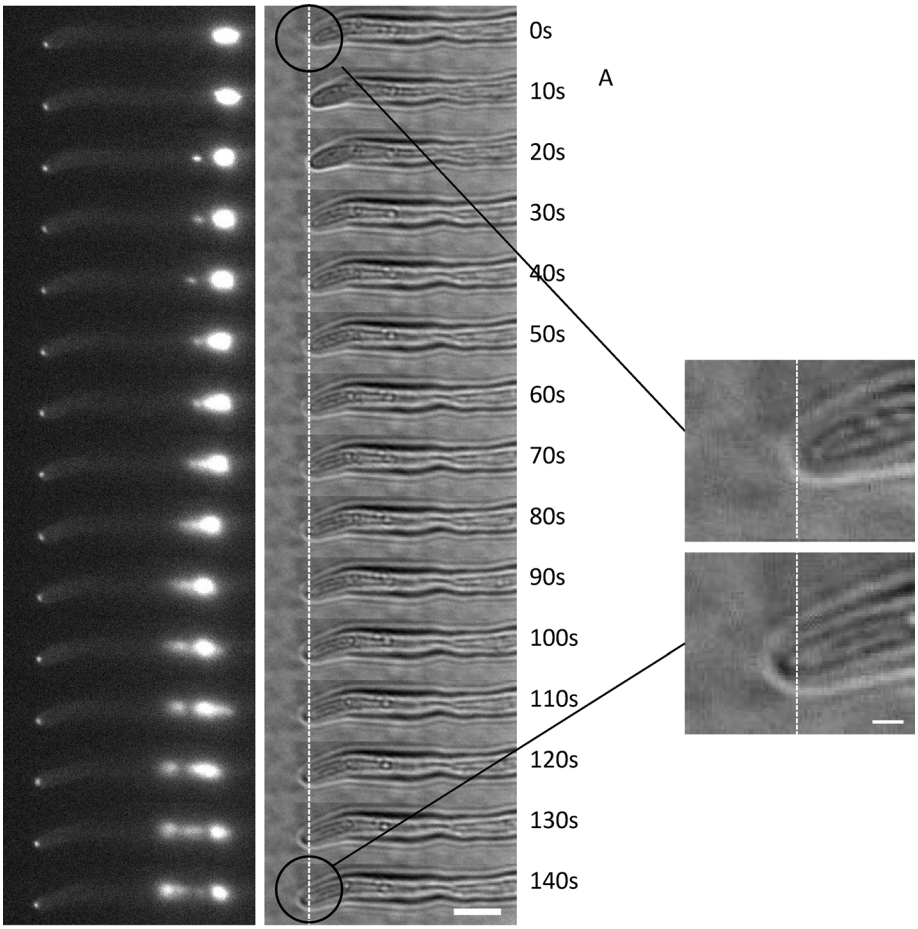

FIGURE 2: Growth does not stop during mitosis. (A) Single frames from Nop1-YFP Mlc1-YFP undergoing mitosis. Images were recorded at 10-s intervals. To reduce phototoxicity and photobleaching, a single Z-plane was recorded at each time point using 50-ms exposure. The full movie is Supplemental Movie S2. Shown here is a montage, generated using the FIJI version of ImageJ, which shows successive images with the initial image starting at frame 43 of the full movie. Left, fluorescence images showing Mlc1-YFP at the hyphal tip and the Nop1-YFP in the nucleus. The satellite spot may represent Mlc1 in the spindle pole body. Right, differential interference contrast images for corresponding fluorescence images at the left. The dashed line is a vertical line dropped from the hyphal tip in the 0-s frame, which reveals the continuous extension of the hyphal tip throughout the image series. The hyphal tip in the initial and final frames is enlarged to show that throughout the 140 s of the image series the tip extends by ~0.8 µm, consistent with the 0.33 µm/min long-term average rate of hyphal growth (Supplemental Figure S1 and Supplemental Movie S1). Scale bar, 5 µm (main images), 1 µm (enlargement). (B) The maximum intensity of the Mlc1 spot in the image series was measured using ImageJ, with the background subtracted, and plotted against time. Units on the ordinate are arbitrary units.

0.33 µm/min (Supplemental Figure S1). Using a combination of FRAP and FLIP, we previously showed that vesicles enter and leave the Spitzenkörper with a turnover time of 30 s (Jones and Sudbery, 2010). The Spitzenkörper remained in place before, during, and after mitosis, and the intensity of Mlc1-YFP did not diminish throughout metaphase and anaphase. This suggests that vesicle traffic into the Spitzenkörper and from the Spitzenkörper to the cell surface continued throughout mitosis. Supplemental Figure S2 shows that throughout mitosis the exocyst component Exo70 also remained as a crescent at the hyphal tip and that the hyphal tip continued to extend. Thus hyphal extension and polarized exocytosis continue throughout mitosis.

Exo84 is phosphorylated by Cdk1 in a hyphal-specific manner

To investigate whether Exo84-YFP is phosphorylated, we looked for a band shift on one-dimensional (1D) PAGE gels before and after λ-phosphatase treatment, using a monoclonal antibody to YFP in a Western blot experiment. Figure 3A shows that Exo84-YFP extracted from exponentially growing yeast cells has a small band shift, whereas Exo84 extracted from hyphae has a larger band shift. To investigate in more detail the pattern of phosphorylation, we fractionated Exo84-YFP using two-dimensional (2D) gels (Figure 2B). Stationary-phase yeast cells show four weak spots, whereas exponentially growing yeast cells show three further spots. Thus Exo84 is phosphorylated under yeast growth conditions consistent with the small band shift we observed in 1D gels. To study the temporal pattern of phosphorylation in hyphal cells, we analyzed samples recovered 30, 60, and 90 min after inoculation into hyphal growth conditions. Exo84 became more phosphorylated, with the spots moving progressively toward the acidic end of the pH range (Figure 3B). By 90 min, three of the additional spots appeared to correspond to the three spots visible in growing yeast, but they are more intense in the hyphal sample. A fourth spot is clearly unique to hyphal growth. Because this is the most acidic, it corresponds to the most highly phosphorylated form of the protein.

C. albicans Exo84 contains three matches to the full Cdk target motif (T/S.P.X.R/K) at positions S256, S384, and T488. Because it is known that Hgc1, the hyphal-specific Cdk1 cyclin, is required for hyphal growth, we examined whether the hyphal-specific band shift depended on the presence of Hgc1. Figure 3, B and C, shows that this is indeed the case. Exo84-YFP extracted from a Δ*hgc*1 strain shows only a slight increase in phosphorylation compared with the stationary phase control in 2D gels (Figure 3B). In 1D gels the band shift observed in wild-type cells was absent in the Δ*hgc*1 strain (Figure 3C).

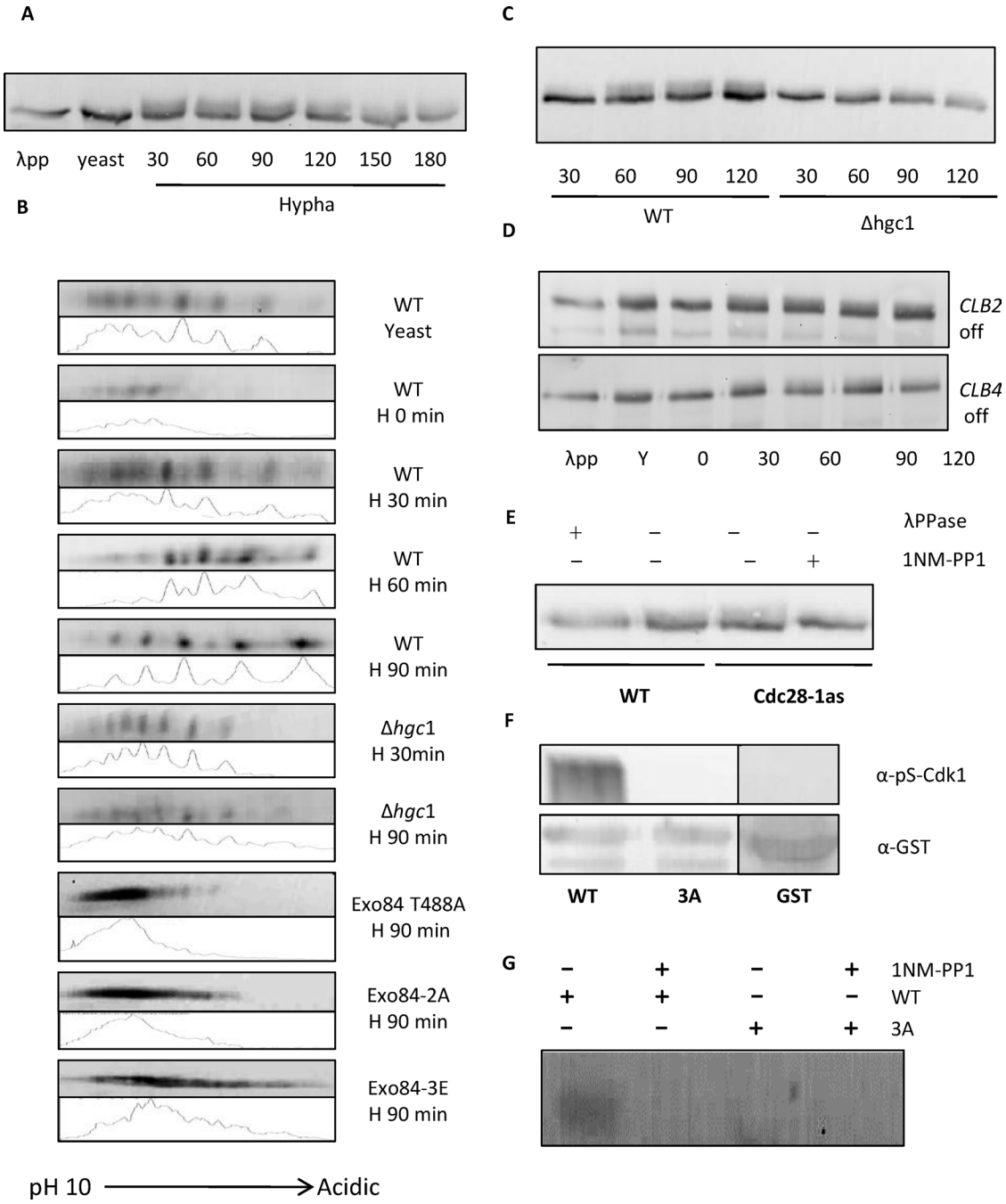

FIGURE 3: Exo84 is phosphorylated by Cdk1. (A) Western blot using anti-GFP antisera of Exo84-YFP from yeast and hyphae as indicated. Numbers indicate time in minutes since unbudded stationary-phase cells were induced to form hyphae. λPP, λ-phosphatase–treated sample. (B) 2D gels of Exo84-YFP from lysates of wild-type (WT) *exo*84 mutant strains as indicated and Δ*hgc*1 strains from WT unbudded stationary-phase cells (WT H 0 min) and from hyphae induced from WT cells after 30, 60, and 90 min and Δ*hgc*1 after 30 and 90 min as indicated. The stationary-phase cells were also reinoculated into yeast growth medium and lysates prepared after 3 h when the cells were in exponential growth (WT Yeast). (C) Exo84 extracted from Δ*hgc*1 cells is less phosphorylated, shown by the absence of the slower-migrating smear present in Exo84 extracted from wild-type cells. (D) Exo84 is still phosphorylated in cells depleted of Clb2 and Clb4. (E) Phosphorylation of Exo84 is inhibited by 1NM-PP1 when the strain carries the *cdk*1-1*as* allele. (F) Recombinant GST-Exo84 but not recombinant GST-Exo84-3A is phosphorylated in vitro by Cdk1. The indicated recombinant forms of GST-Exo-84 or GST alone were incubated in kinase reaction buffer with immunoprecipitated Cdk1-HA. The products were analyzed on a Western blot using the anti–pS-Cdk1 antibody. (G) The in vitro kinase reaction is inhibited by 1NM PP1 when the purified kinase carries the analogue-sensitive cdk1-1as allele.

In *S. cerevisiae* Cdk1 partnered by Clb2 phosphorylates Exo84 to arrest cell growth during mitosis (Luo *et al.*, 2013). Because deletion of Clb2 is lethal in *C. albicans*, we used a strain in which Clb2 was expressed from the regulatable *MET*3 promoter to investigate its possible involvement (Bensen *et al.*, 2005). When yeast cells were grown with the *MET*3 promoter repressed, cells arrested with an

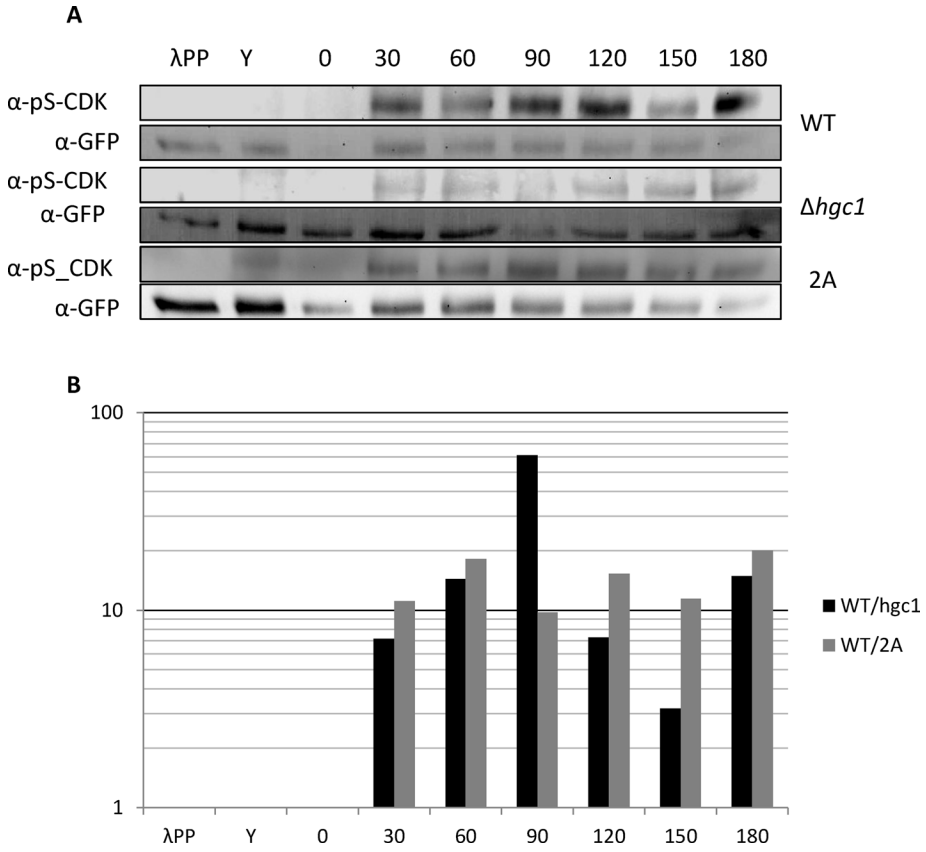

FIGURE 4: Phosphorylation of Exo84-YFP detected by the anti–pS-Cdk1 antibody is reduced in Exo84-2A or in cells lacking Hgc1. (A) Membranes were stripped and reprobed with an anti-GFP antibody as a loading control. (B) Ratios of the wild-type to mutant intensities of the anti–pS-Cdk1 signals normalized by the GFP loading controls.

elongated phenotype, as previously reported, confirming that Clb2 was successfully depleted. We found that hyphae induced in the absence of Clb2 arrested after the first nuclear division and showed no change in Exo84 phosphorylation (Figure 3D). Similarly, we found no change in phosphorylation of Exo84-YFP when *CLB4* expression was repressed in a *MET3-CLB4* strain (Bensen *et al.*, 2005; Figure 3D). Thus phosphorylation of Exo84 is dependent on Cdk1 partnered by Hgc1.

To further confirm the requirement for Cdk1, we examined whether the band shift was present when a strain expressing only the analogue-sensitive Cdk1-as1 allele was inhibited by the presence of 1NM-PP1. As shown in Figure 3E, the hyphal-specific band shift disappeared in the presence of 1NM-PP1. To investigate whether Cdk1 directly phosphorylates Exo84, we carried out an in vitro kinase assay with recombinant GST-Exo84 as the substrate and Cdk1 purified from *C. albicans* hyphae. To monitor the reaction, we used an antibody specific to phosphorylated serine in the full motif recognized by cyclin-dependent kinases (S.P.X.R/K; hereafter referred to as anti–pS-Cdk). Recombinant wild-type Exo84 was phosphorylated by purified Cdk1, but recombinant GST-Exo84 in which the three Cdk target sites had been substituted by alanine (Exo84-3A) was not a substrate (Figure 3F). To demonstrate that the active kinase was Cdk1 and not a copurifying kinase, we repeated the experiment using purified Cdk1-as1 carrying the analogue-sensitive allele. As we found previously (Bishop *et al.*, 2010), this kinase shows lower activity in vitro even in the absence of inhibitor, suggesting that it is not fully active. Nevertheless it is clear that in the absence but not the presence of 1NM-PP1, Exo84 is phosphorylated in vitro, demonstrating that the active kinase is Cdk1 (Figure 3G).

We used the anti–pS-Cdk antibody to investigate the pattern of Cdk1-specific phosphorylation of Exo84 in vivo (Figure 4). Exo84 extracted from wild-type cells reacted strongly with this antibody from 30 min after hyphal induction onward. Exo84 extracted from Δ*hgc*1 cells showed strongly reduced phosphorylation, consistent with the conclusion that Cdk1-Hgc1 is targeting Exo84. To confirm that the three full Cdk1 targets are involved, we constructed mutants in which these sites were mutated (described in more detail later). The strain in which all of the three Cdk1 target sites were mutated to alanine (Exo84-3A) was barely viable, producing slow-growing yeast cells that were greatly enlarged and failed to show any polarized growth in response to hyphal-inducing cues. We did not characterize this strain further. The strain in which both S256 and S384 were mutated to alanine (Exo84-2A) showed significant hyphal defects, as we document later. In a Western blot using the anti–pS-Cdk antibody, Exo84-2A showed significantly less phosphorylation than the wild type (Figure 4). We also used 2D gels to examine the pattern of phosphorylation during hyphal growth in Exo84-2A and two further mutants: one with a nonphosphorylatable alanine substitution at residue T488 (Exo84-T488A), and Exo84-3E, where the three putative phospho-acceptor sites had been mutated to phosphomimetic glutamate. In these 2D gels, in both Exo84-2A and Exo84-T488A, proteins showed reduced phosphorylation, consistent with these residues being the target of Cdk1-Hgc1 (Figure 3B). However, it was not possible to associate any particular residue with the discrete spots observed in the 2D gel of wild-type Exo84 extracted from hyphal-grown cells. Exo84-3E showed a shift toward the acidic end of the pH range, consistent with the increased negative charge of the glutamate residues.

Phosphorylation of Exo84 is required for the highly polarized growth of hyphae

To investigate the physiological role of Exo84 phosphorylation, we first confirmed that Exo84 is essential in *C. albicans*. In the diploid genome of *C. albicans* the upstream sequence of Exo84 is different in the two alleles. A retrotransponson of the Gypsy group is inserted 79 base pairs upstream of allele Orf19.135, whereas in allele Orf19.7779, the 3′ end of *SIF*2 (Orf19.7778) is located 236 base pairs upstream of the start of the *EXO*84 open reading frame (ORF). Deletion of either *EXO*84 ORF has no major phenotypic effect; thus both alleles are functional and haplosufficient. When the remaining allele is placed under control of the regulatable *MAL2* promoter, cells are unable to grow on glucose, which represses the *MAL2* promoter (Supplemental Figure S3A). Thus Exo84 is essential. Depletion of Exo84 results in round, enlarged cells with wide necks and with some cells containing multiple nuclei, suggesting that Exo84 is required for polarized growth and cytokinesis, as it is in *S. cerevisiae* (Supplemental Figure S3B).

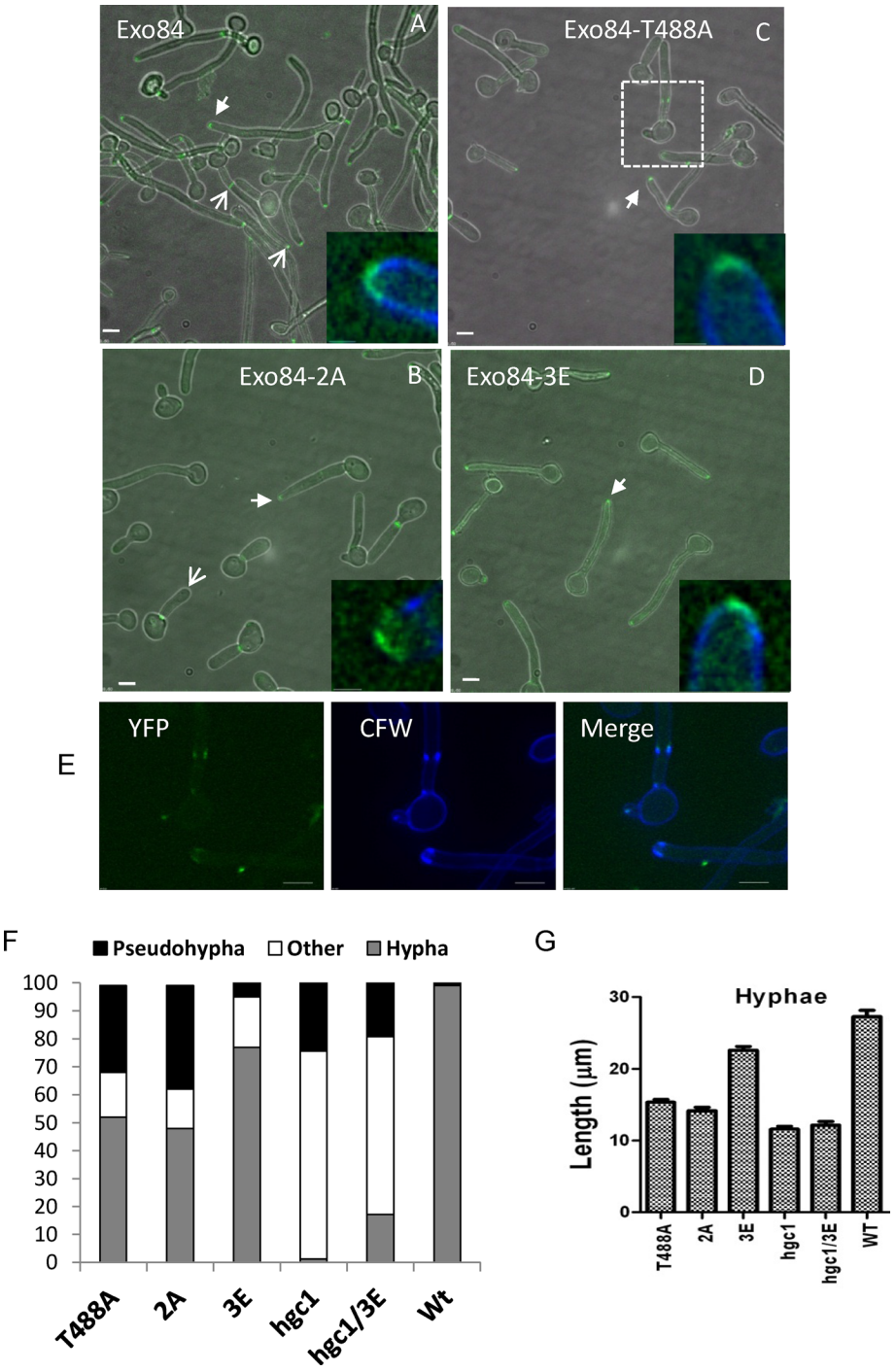

FIGURE 5: Phenotype of cells expressing nonphosphorylatable or phosphomimetic substitutions. (A–D) Appearance of cells expressing the indicated proteins fused to YFP 120 min after hyphae were induced from unbudded stationary-phase yeast cells. Cells were harvested and resuspended in PBS containing calcofluor white (CFW). The main images show the merged YFP–differential interference contrast channels. Insets show enlargements of the merged YFP and blue CFW channels of the tips indicated by solid arrows (pixilation in the inset images was smoothed with Softworx interpolated zoom function). (A) Barbed arrows indicate a hypha where YFP is simultaneously present at the tip and septum. (B) Barbed arrow indicates a pseudohypha with YFP at the septum but not the tip. Scale bars, 5 µm (main image), 1 µm (insets). (E) Enlargement of the YFP, CFW, and merged images in the area bounded by dashed lines in C. Scale bars, 5 µm. (F) Quantitation of morphology of the indicated strains 120 min after hyphal induction was carried out based on criteria described previously (Sudbery *et al.*, 2004). Cells were classified as hyphae when the daughter compartment was narrow (<2 µm) and had parallel sides and CFW staining (not shown) showed that the first septum was within the germ tube. Cells were classified as pseudohyphae when the width was >2 µm, there was a constriction and a septum at the neck of the mother cell–daughter compartment, and the sides were not parallel. Cells were classified as "other" when a short, parallel-sided germ tube swelled to form a less-polarized compartment. A minimum of 150 cells was classified for each strain. (G) The length of the hyphal compartment measured in the same cells.

We constructed strains in which the only copy of Exo84 carried nonphosphorylatable alanine substitutions at each of the putative Cdk1 phosphorylation sites (Exo84-S256A, Exo84-S384A, Exo84-T488A). We combined the mutations to make double (Exo84-S256A S384A) and triple (Exo84-S256A S384A T488A) mutants, hereafter called Exo84-2A and Exo84-3A, respectively. We also constructed phosphomimetic substitutions at the T488 site (Exo84-T488E) and at all three putative sites (Exo84-S256E S384E T488E), hereafter called Exo84-3E. All of these strains were constructed with C-terminal YFP fusions. Fusing the remaining copy of *EXO84* in the heterozygous strain to YFP had no phenotypic consequences; thus the Exo84-YFP is a functional protein. We carried out Western blots using an anti-GFP antibody, which confirmed that each of these proteins was present in amount comparable to the wild-type level (unpublished data).

As described earlier, the strain expressing only Exo84-3A was severely affected, and we did not characterize this strain further. The Exo84-2A strain showed significant morphological abnormities in the hyphal form compared with wild type (Figure 5, A and B). Quantitation showed that there was a significant increase in the number of pseudohyphal cells compared with wild type (Figure 5F), and in addition some hyphae showed a phenotype similar to the Δ*hgc*1 phenotype, that is, a short, normal-appearing germ tube, which quickly reverted to less polarized growth resembling pseudohyphae. We refer to these cells as "other" since they resemble neither hyphae nor pseudohyphae. Although a significant proportion of Exo84-2A cells made hyphae that were morphologically normal, these hyphae were extended at approximately half the rate of wild-type hyphae (Figure 5G). Thus phosphorylation of Exo84 is necessary to allow the highly polarized growth characteristic of hyphae. The strain expressing only the *EXO84* T488A allele was similarly affected, showing marked reduction in the proportion of cells showing normal hyphal morphology (Figure 5, D and F). Again, where cells formed morphologically normal

hyphae, these hyphae extended at a markedly slower rate than the wild-type cells (Figure 5G). The strain carrying the *EXO*84-S384A allele also showed a reduction in the proportion of hyphal cells, and the hyphae that did form extended more slowly. However, this reduction was less extreme than for the *EXO*84-2A and *EXO*84 T488A strains (unpublished data). The *EXO*84-S256A allele did not have a significant effect on cell morphology or hyphal extension rate (unpublished data).

The fusion of Exo84 to YFP in the wild-type and mutant proteins allowed us to investigate the localization of Exo84. As we described previously, Exo84-YFP localizes to a surface crescent in wild-type hyphae (Figure 5, A and inset). Exo84 is also present at the septum site during cytokinesis to promote the polarized growth necessary for the formation of secondary cell walls (Figure 5A, barbed arrows). In the Exo84-2A mutant cells, Exo84-2A-YFP localized to a crescent at the tip of hyphal cells (Figure 5, B and inset). However, in cells growing in the pseudohyphal phenotype, Exo84-2A-YFP relocated to the septum late in the cell cycle and was no longer present at the tip (Figure 5B, barbed arrow), consistent with our previous report that polarity components relocate from the tip of pseudohyphal cells late in the cell cycle (Crampin *et al.*, 2005). Exo84-T488A-YFP also localized to the tip of hyphal cells (Figure 5, C and inset) and, like Exo84-2A-YFP, was present at the tip or septum of pseudohyphal cells but not at both simultaneously. Figure 5, C and E, illustrates a phenomenon that we also occasionally observed in the Exo84-2A mutants. As can be seen in the region enlarged in Figure 5E, Exo84 becomes ectopically located with diffuse localization at the tip and an incomplete ring at the septum. Calcofluor white staining reveals that this ectopic localization is associated with excess chitin deposition. In the yeast form both the Exo84-2A and the Exo84-T488A strains showed an increase in mother cell volume compared with wild-type yeast cells (Supplemental Figure S4). However, the axial ratio (major/minor axis) was reduced, showing that cells were rounder than wild-type cells.

In hyphal-promoting growth conditions, cells expressing the phosphomimetic Exo84-3E allele were more similar to wild-type cells than cells expressing nonphosphorylatable alleles (Figure 5D). There was a smaller reduction in the proportion of cells that formed true hyphae (Figure 5F) and a smaller reduction in the rate of hyphal extension (Figure 5G). Exo84-3E yeast cells showed an increase in cell volume compared with wild-type yeast cells, but the axial ratio was not significantly different, showing that cell shape was not altered (Supplemental Figure S4). Of interest, the *Exo*84-T488E allele showed a decrease in cell volume and an increased axial ratio, suggesting a longer or more pronounced phase of polarized growth during their cell cycles (Supplemental Figure S4).

Whereas nonphosphorylatable alanine substitutions at the Cdk1 target sites impair polarized growth and hyphal morphology, phosphomimetic substitutions have only a mild effect on the hyphal phenotype. This is consistent with the hypothesis that phosphorylation of Exo84 is necessary for the extreme polarized growth of hyphae. If one of the roles of Hgc1-Cdk1 is to phosphorylate Exo84, then it is possible that the Exo-84-3E allele may alleviate some or all of the phenotypic effects of the Δ*hgc*1 allele. To test this idea, we constructed a Δ*hgc*1 *EXO*84-3E strain. The *EXO*84-3E allele did not rescue the phenotype of the Δ*hgc*1 allele. However, there was an increase in the proportion of hyphal cells from 1.2 to 17% (Figure 5F). Because other functions of Hgc1-Cdc28 have been documented, it is not surprising that the *EXO*84-3E allele does not fully rescue the effects of a Δ*hgc*1 mutation. One such target of Hgc1-Cdk1 is Rga2, which acts as a negative regulator of hyphal growth that is relieved upon phosphorylation (Zheng *et al.*, 2007). We previously showed that although deletion of Rga2 does not induce constitutive hyphal growth, hyphal growth is initiated in Δ*rga2* mutants under conditions that would normally induce pseudohyphal formation (Court and Sudbery, 2007). We thus investigated whether the Exo84-3E mutant also increased the proportion hyphae when cells were grown at 35°C and pH 6.0, which would normally induce pseudohyphal growth (Figure 6). Indeed, under these conditions the proportion of hyphae increased from 15% in wild-type cells to 35% in Exo84-3E mutants. In contrast, hyphal growth was absent (Exo84-T488A) or nearly absent (Exo84-2A) in the nonphosphorylatable mutant alleles (Figure 6). Taken together, these experiments provide further support for the hypothesis that Hgc1-Cdk1 targets Exo84 at the three full consensus Cdk1 target sites to promote hyphal growth, although it is clear that Cdk1 also has other targets that must be phosphorylated for the full hyphal phenotype.

When hyphae are able to form, phosphorylation of Exo84 is not required for its localization or exocyst assembly

Exo84 is continuously present as a surface crescent at the tip of hyphae, and during cytokinesis it is simultaneously present at the site of septum formation and the hyphal tip (Figures 5A). The morphological defects resulting from the mutant alleles described earlier were observed in cells growing on rich yeast extract/peptone/glucose (YEPD) medium. We found that the morphological defects of the *exo*84-2A and *exo*84-T488A alleles were less pronounced on minimal medium, so that a higher proportion had a hyphal morphology (Figure 7A). Nevertheless, these hyphae extended at a slower rate than wild-type hyphae, showing that the nonphosphorylatable alleles still reduced polarized growth. We took advantage of this observation to investigate whether the mutations affected the location of Exo84 to sites of septum formation during hyphal growth. We followed Exo84-YFP localization over time in wild-type cells and strains carrying each of the nonphosphorylatable and phosphomimetic alleles fused to YFP. Figure 7B shows the percentage of cells displaying Exo84 in the septum plotted against time after hyphal induction. In wild-type cells a peak of septum-located Exo84 occurs at 115 min. Cumulatively, Exo84 was observed at the septum in 70% of wild-type hyphae by 150 min (Figure 7C). Mutant cells that formed hyphae also showed localization of Exo84 to the septum (Figure 7A). However, it is observed at a later time in the septum compared with wild-type cells, and the cumulative proportion of cells that displayed septum-located Exo84 is much lower in each of the mutants (Figure 7C). However, when Exo84 is present at the septum, the total length of the hypha and the distance from the bud neck to the septum is similar in the wild type and mutants (Figure 7D). This suggests that the delay in Exo84 location to the septum reflects an increased time to reach a critical hyphal length at which cytokinesis is initiated due to the lower extension rate of the hyphae. Thus in these hyphal cells the presence or absence of phosphorylation does not affect Exo84 localization but does affect the rate of polarized growth.

In *S. cerevisiae*, phosphorylation of Exo84 disrupts the assembly of the exocyst complex (Luo *et al.*, 2013). We showed (Supplemental Figure S2) that Exo70 remains at the bud tip throughout mitosis. To further investigate the effect of Exo84 phosphorylation on exocyst interactions, we examined whether phosphorylation of Exo84 affected its interaction with Sec10, as this interaction is disrupted in *S. cerevisiae* by Exo84 phosphorylation. We constructed Exo84-GFP Sec10-HA strains in which Exo84 was wild type or carried respectively the Exo84-T488A, Exo84-2A, and 3E mutations. Using these strains, we carried out reciprocal immunoprecipitation experiments. In each case the mutations did not affect the interaction of Exo84 and Sec10 (Figure 8, A and B).

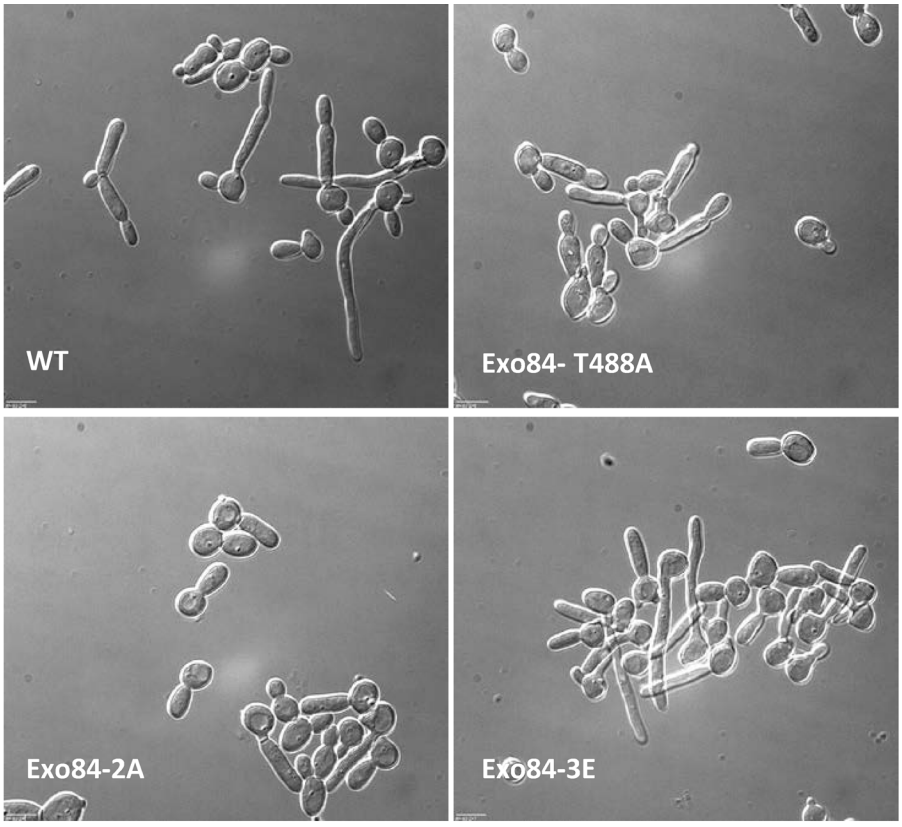

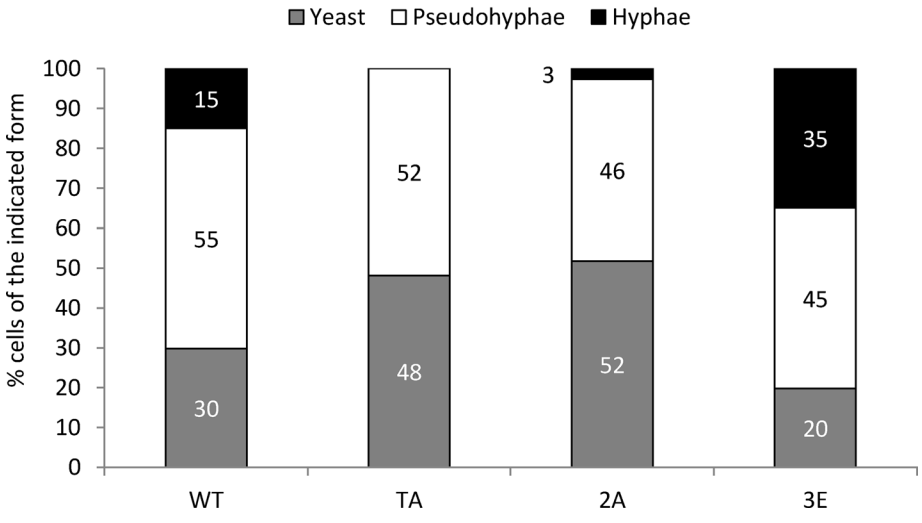

FIGURE 6: The phosphomimetic *EXO*84-3E allele promotes hyphal growth under pseudohyphal growth conditions. Stationary-phase cells were inoculated into YEPD, pH 6.0, and cultured at 35°C. Morphology was classified as described in the legend to Figure 5. A minimum of 150 cells was classified for each strain.

Phosphorylation of Exo84 may affect phospholipid binding

Exo84 contains a PH domain that promotes interactions between proteins and phospholipids (Figure 1A). The S384 site is located within this domain, whereas protein threading suggests that the important S256 and T488 sites are on either side of this domain in the folded protein (Figure 1A). We therefore investigated whether Exo84 binds phospholipids, and if so, whether phosphorylation Exo84 affects the binding. To do this, we used a PIP strip and recombinant GST-Exo84 and GST-Exo84-3E (Figure 9A). Wild-type GST-Exo84 appeared to have the greatest affinity for phosphatidylserine (PS), with a much weaker affinity for phosphatidic acid (Figure 9, A and B). Because this protein was expressed in *Escherichia coli*, it is not phosphorylated, and so this reports the affinity of the nonphosphorylated form of the protein. Of interest, the GST-Exo84-3E protein appeared to have a considerably reduced affinity for PS, consistent with the negative charge on PS and the increased negative charge on Exo84 resulting from the phosphorylation (Figure 9, A and B) Note that 8 µg of recombinant Exo84-3E but only 2 µg of recombinant Exo84 were loaded onto each spot in the PIP strip; thus the reduced affinity of Exo84 for PS is likely to be considerably greater than the 2.5-fold reduction in Figure 9A.

PS is synthesized from cytidyldiphosphate-diacylglycerol and serine by the action of phosphatidylserine synthase, encoded by the *CHO*1 gene (Chen *et al.*, 2010). In *C. albicans*, Δ*cho*1 mutants are viable but have cell wall defects and fail to show filamentous growth on Spider medium. In addition, they are auxotrophic for ethanolamine, as phosphatidylethanolamine is synthesized from PS. To investigate further whether PS plays a role in Exo84 localization, we constructed a Δ*cho*1 Exo84-YFP strain and investigated its phenotype. We used defined medium supplemented with phosphatidylethanolamine, since we found that YEPD contained sufficient PS to supplement the PS auxotrophy. On defined medium this strain grew slowly. In both wild-type and Δ*cho*1 yeast cells Exo84-YFP localized to the septum and the tip of small buds (Figures 7A and 9C). During hyphal growth in Δ*cho*1 cells (induced on Lee's medium; Lee *et al.*, 1975), Exo84 also showed a disturbed pattern of localization, so that although it was present at the tip, it was also present in ectopic sites in the mother cell and within the germ tube (Figure 9C). As a control, we also constructed a Δ*cho*1 strain expressing Sec3-YFP, which during both yeast and hyphae growth did not show the ectopic localization. (Figure 9C). Thus ectopic localization of Exo84 in the absence of PS is specific to Exo84 is not a caused by a general failure of exocyst localization.

Although these observations suggest a role for PS in the localization of Exo84, the role of this phosphorylation is not straightforward because phosphorylation lowers the affinity of Exo84 for PS. It may be that the phosphorylation is important to dissociate Exo84 from membranes to allow it to be recycled to the growing tip in a manner reminiscent of recent models of the role of endocytosis in restricting

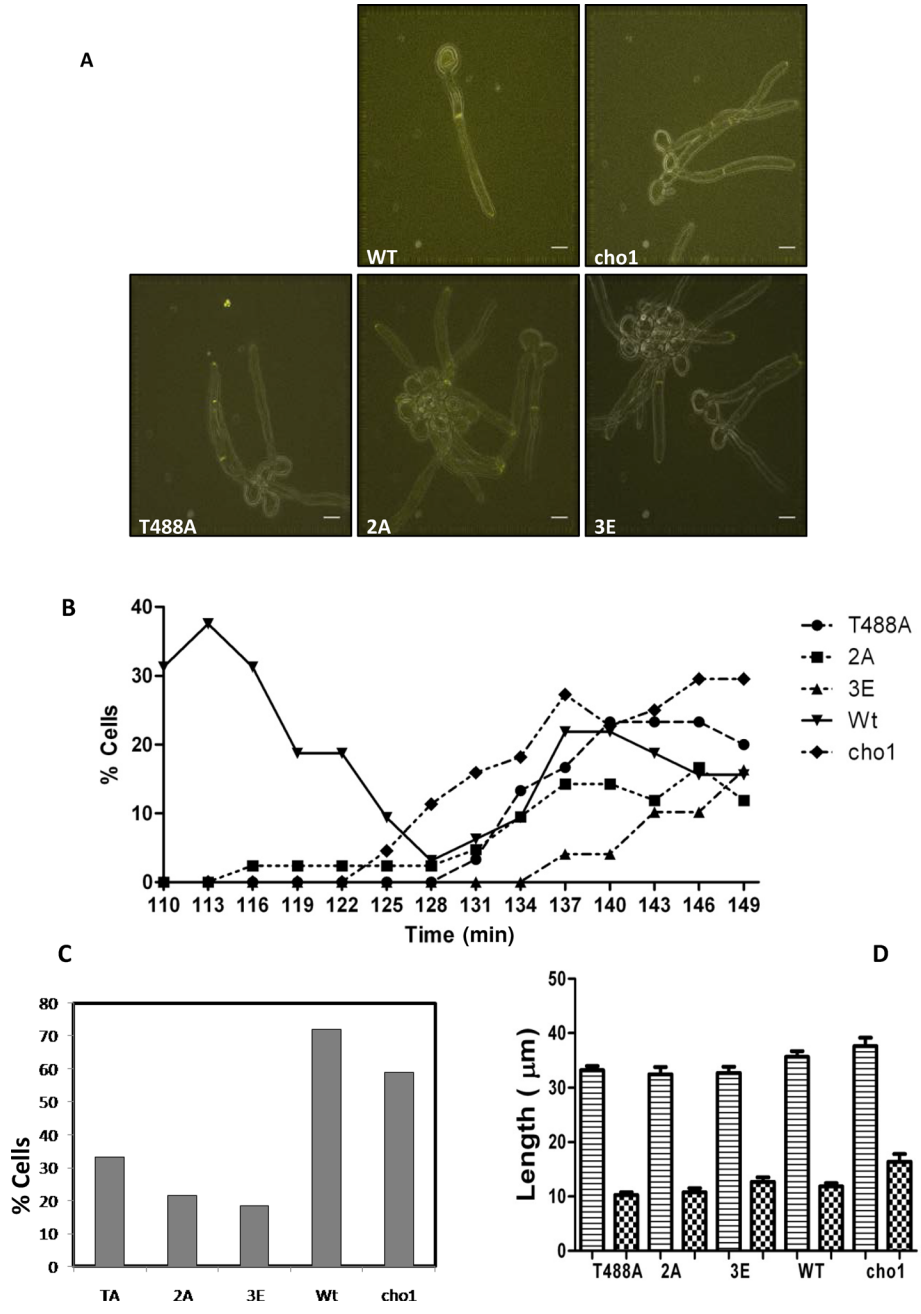

FIGURE 7: Effect of Exo84 phosphoacceptor-site mutations on the localization of Exo84-YFP in hyphal cells. Individual cells of the indicated strains were grown on agar pads containing minimal medium as described previously (Bishop *et al.*, 2010), and at 3-min intervals each cell was examined to determine whether Exo84-YFP had located to the septum. (A) Appearance of cells where Exo84 is present at the tip and septum. The image is a merge image of the YFP fluorescence and the differential interference contrast (DIC) images, where the contrast of the DIC images has been increased to generate a cell outline. (B) The percentage of cells showing Exo84 at the septum plotted against time after hyphal induction. At least 10 cells were examined simultaneously for each strain. (C) Cumulative total of cells where Exo84 appeared at the septum after 150 min. (D) Length of the hypha when Exo84 first appeared at the septum for each strain (horizontal hatch) and the distance of the septum from the bud neck (hatched bars). The relevance of the Δ*cho1* mutant is described in the section *Phosphorylation of Exo84 may affect phospholipid binding*.

localization of Cdc42 to sites of polarized growth. To address this possibility, we examined the recycling kinetics of Exo84-2A and Exo84-3E using FRAP. To avoid the application of extensive bleaching corrections during postbleach imaging, we used an experimental design we developed previously in which we measured the fraction of fluorescence recovered in 30 s (Jones and Sudbery, 2010). Exo84-2A-YFP recovered only 35% of the prebleach fluorescence in 30 s, whereas wild-type Exo84-YFP recovered 53%, a difference that was statistically significant (Figure 10). Exo84-3E recovered 60% of prebleach fluorescence. Although this was more than the wild-type protein, the difference was not significant. Thus phosphorylation of Exo84 is necessary for the rapid exchange of Exo84 at the cell surface, consistent with the idea that phosphorylation promotes Exo84 recycling by promoting its dissociation from PS.

DISCUSSION

During the growth of a bud in *S. cerevisiae* or the yeast phase of *C. albicans*, growth is polarized for a short period as the bud emerges but later becomes isotropic around the whole of the bud perimeter. The period of polarized growth relative to isotropic growth must be relatively short because, as we record here, the axial ratio of the prolate spheroid *C. albicans* cells is 1.5. During cytokinesis, polarized growth relocates to the site of septum formation. However, it was recently shown in *S. cerevisiae* that fusion of secretory vesicles is blocked during metaphase, and cell surface expansion ceases (Luo *et al.*, 2013). *C. albicans* hyphae show a radically different pattern of growth than the yeast phase. Polarized growth is focused to a narrow area at the hyphal tip and is continuous throughout the whole cell cycle. It does not show the polarized-to-isotropic switch, and we show here that it does not cease at any point during mitosis or cytokinesis. Despite this radically different growth pattern, studies on the mechanism of polarized growth in *C. albicans* suggest that the same components are used as elaborated in the *S. cerevisiae* budding yeast model (for review see Sudbery, 2011). Clearly, however, the machinery must be modified to produce the radically different outcome of hyphal growth.

Here we uncovered one of the key differences. In *C. albicans* the exocyst component Exo84 is phosphorylated by Cdk1 as it is in *S. cerevisiae*. However, instead of causing the disassembly of the exocyst complex and halting the fusion of secretory vesicles necessary for cell surface expansion, phosphorylation of Exo84 in *C. albicans* is necessary for the efficient polarized growth of hyphae. Substitutions of nonphosphorylatable residues at the consensus Cdk1 phosphorylation sites cause morphological abnormalities in many cells growing on rich medium and reduces hyphal extension rates on all media. The morphological abnormalities include an

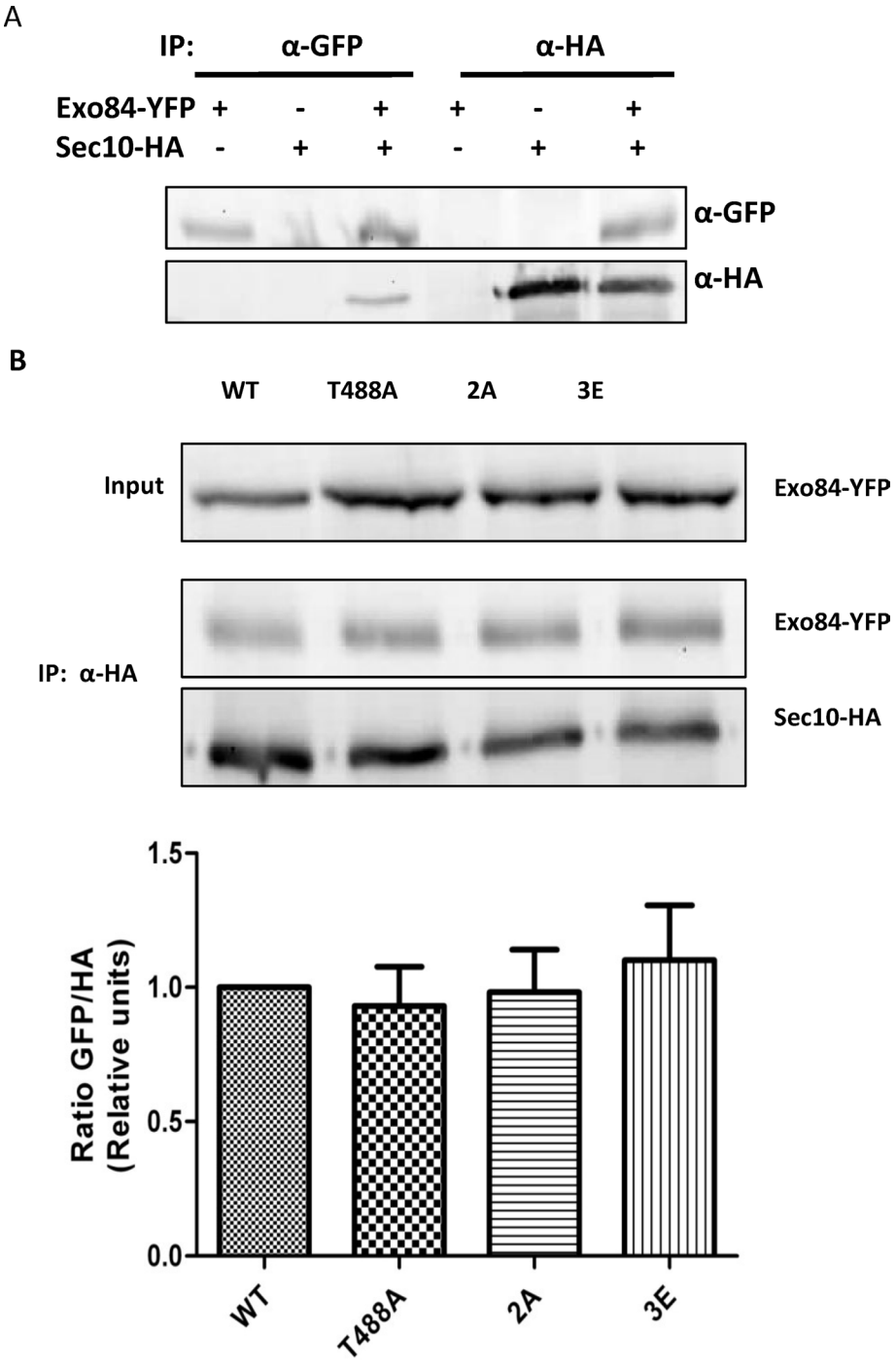

FIGURE 8: Exo84 phospho-site mutations do not disrupt the association with Sec10. (A) Reciprocal immunoprecipitation of Exo84-YFP with Sec10-HA. (B) Immunoprecipitation of Sec10-HA with Exo84-YFP carrying the indicated mutations. Controls in A show that the anti-GFP and anti-HA antibodies do not show nonspecific interactions.

increased proportion of cells that grow as pseudohyphae, as well as cells that resemble the Δ*hgc*1 phenotype, where cells evaginate germ tubes that that appear normal but quickly revert to the less-polarized growth typical of pseudohyphae. These abnormalities are not shown by cells carrying phosphomimetic substitutions at the same sites. In particular, whereas the Exo84-3A mutant is severely affected and in many ways resembles the phenotype of cells depleted of Exo84, the Exo84-3E strain shows only minor abnormalities.

We also observed that Exo84 is phosphorylated during yeast-phase growth, although this was not as extensive as hyphal growth. Exo84 phosphorylation is clearly important for yeast growth, as shown by the major effect of the Exo84-3A allele in the yeast-phase phenotype; moreover, the mother cells of Exo84-3A, Exo84-2A, and Exo84-T488A strains were rounder than the wild type. This suggests that Exo84 phosphorylation is required for the initial polarized growth of small yeast buds. Intriguingly, it was previously reported that *S. cerevisiae* cells arrested at Start by *cdc*28-4 and *cdc*7-1 alleles at 37°C show increased affinity of Exo84 for other components of the exocyst (Luo *et al.*, 2013). In addition, Exo84 shows a weak reaction to the antibody recognizing phosphorylated Cdk1 target sites in cells arrested at start by α-factor. Such cells form mating projections that have many similarities to hyphae (Chapa-Y-Lazo *et al.*, 2011). Finally, the Cln2-Cdk1 kinase phosphorylates recombinant Exo84 in vitro (Luo *et al.*, 2013). Taken together, these observations suggest that phosphorylation of Exo84 may also play a role in polarized growth in *S. cerevisiae*.

What is the role of Exo84 phosphorylation? One of the Cdk sites is within the PH domain, and the other two sites are located on either side of the PH domain in the 3D model of the protein reconstructed by threading analysis (Figure 1A). PH domains bind phospholipids in membranes, and we show here that recombinant GST-Exo84, which is not phosphorylated, has an affinity for PS and that this is reduced in the Exo83-3E, which mimics a fully phosphorylated protein. Thus phosphorylation may regulate the affinity of Exo84 for this phospholipid. A precedent for the role of PS in polarized growth is the demonstration that in *S. cerevisiae* it is localized to sites of polarized growth and facilitates recruitment of Cdc42-GTP to these sites. We showed that in Δ*cho*1 cells, which are unable to synthesize PS, Exo84 localized ectopically to punctate patches at the cell surface in both yeast and hyphae. Nevertheless, in these cells Exo84 also localizes to sites of polarized growth such as the tip of small buds and the septum in yeast, and the hyphal tip and septum in hyphae. Thus loss of PS lowers the efficiency of, but does not completely prevent, Exo84 localization. In *S. cerevisiae*, Sec3 is believed to provide a landmark for exocyst assembly. In *C. albicans*, ΔSec3 cells fail to maintain polarized growth after the formation of the first septum, a phenotype that depends on the presence of Cdc11 in the septin ring (Li *et al.*, 2007). In *C. albicans* Δ*cho*1 cells, Sec3 localizes normally to the septum, showing that the inefficient localization of Exo84 in Δ*cho*1 cells is specific and not due to general disorganization of the polarity machinery. A possible role for the phosphorylation is that it promotes

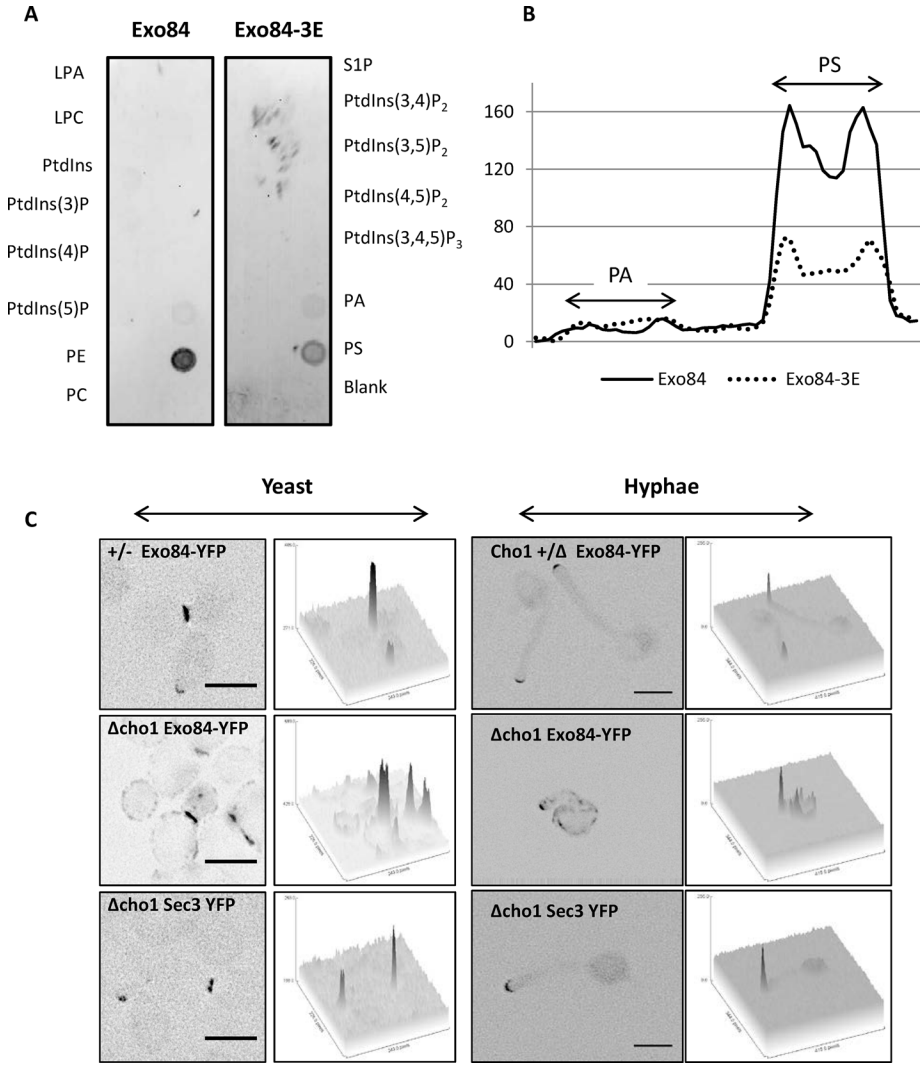

FIGURE 9: Exo84 interacts with phosphatidylserine. (A) Binding of Exo84 to phospholipids. We incubated 2 µg of recombinant GST-Exo84 and 8 µg of GST-Exo84-3E with the phospholipid test strip. The phospholipids on the PIP strip are organized in two columns. Left column is labeled to the left of the Exo84 strip, and right column is labeled to the right of the Exo84-3E strip. LPA, lysophosphatidic acid; LPC, lysophosphocholine; PA, phosphatidic acid; PC, phosphatidylcholine; PE, phosphatidylethanolamine; PS, phosphatidylserine; PtpIns, phosphoinositol; SIP, sphingosine-1-phosphate. (B) Profile of Exo84 and Exo84-3E binding to PA and PS on a PIP strip with the background subtracted. Units on the ordinate are arbitrary units. (C) Exo84-YFP and Sec3-YFP distribution in heterozygous *CHO1*/Δ*cho1* and Δ*cho* yeast and hyphal cells as indicated. Three-dimensional quantitation of fluorescence intensity is presented alongside each fluorescence image, which has been color inverted for clarity.

Exo84 recycling by lowering its affinity for PS. Its reduced rate of fluorescence recovery after photobleaching is consistent with this idea.

In conclusion, the special growth characteristics of *C. albicans* hyphae revealed a previously hidden role for Exo84 phosphorylation by a cyclin-dependent kinase. Rather than causing cell surface expansion to cease during mitosis, phosphorylation is necessary for the efficient polarized growth of hyphae, possibly by altering Exo84 affinity for PS in the cell membrane. The different actions on Exo84 of Cdk1-Hgc1 in *C. albicans* and Cdk1-Clb2 in *S.* cerevisiae are consistent with the different patterns of the Cdk1 target sites in the two proteins. *Ca*Exo84 contains a Cdk1 phosphorylation site in the PH domain, explaining the reduction in its affinity for PS, whereas *Sc*Exo84 contains a phosphorylation site in the C-terminal interaction domain, explaining the loss of interaction with other exocyst subunits. Thus, whereas *EXO84* is present in the genomes of both species, it has evolved so that its phosphorylation adapts each organism to its particular pattern of growth

MATERIALS AND METHODS

Media and growth conditions

YEPD consists of 2% glucose, 2% Bacto peptone (Difco), and 1% Bacto yeast extract (Difco) plus 80 mg/l uridine. SD medium consists of 0.67% (wt/vol) yeast nitrogen base (Difco), 2% (wt/vol) glucose, 80 mg/l uridine or 40 mg/l histidine, and arginine. Hyphae were induced from unbudded stationary-phase yeast cells as described previously. The Δ*cho*1 mutant was grown in synthetic defined (SD) medium containing 1 mM ethanolamine, and hyphal growth was induced in Lee's medium (Lee *et al.*, 1975). Shutdown of p*MET3-CLB2* experiments was carried out in SD supplemented with 10 mM methionine and 2.5 mM cysteine.

Strain and plasmid constructions

Strains constructed are listed in Supplemental Table S1, and the oligonucleotides used are listed in Supplemental Table S2. All strains were derived from BWP17 (Wilson *et al.*, 1999). Gene deletions and C-terminal YFP fusions and hemagglutinin (HA) fusions were performed as previously described (Gola *et al.*, 2003; Schaub *et al.*, 2006; Lavoie *et al.*, 2008; Walther and Wendland, 2008). All strains were checked for correct genome integration by PCR. Correct expression of protein fusion strains was also verified by Western blot using antibodies to the fusion protein or epitope (unpublished data).

Generation of *EXO84* mutant alleles was carried out as described previously (Court and Sudbery, 2007).

Western blots

Western blots were carried out as described previously (Wightman *et al.*, 2004).

2D gel electrophoresis

Exo84-YFP was immunoprecipitated as previously described and then eluted from beads with hydration buffer (8 mM urea, 2 M thiourea, 4% 3-[(3-cholamidopropyl)dimethylammonio]-1-propanesulfonate, 1 mM dithiothreitol [DTT], 0.5% IPG buffer, pH 3–10, and 1.2% DeStreak Reagent; GE Healthcare). The immunoprecipitated protein was resolved on 2D gels using 7-cm Immobiline Drystrip, pH 3–10, and the Ettan IPGphor 3 Isoelectric Focusing System (GE Healthcare).

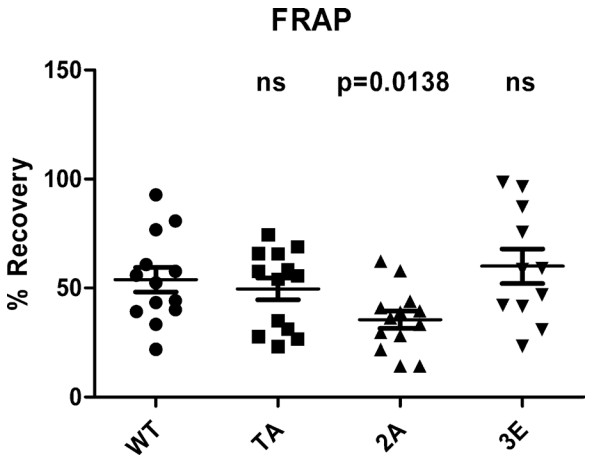

FIGURE 10: Nonphosphorylatable substitutions reduce Exo84-YFP recovery after photobleaching. The indicated strains were grown as hyphae on agar pads in a DeltaVision microscope (TA, Exo84-EXO84 T488A). The tips were bleached using a laser. Images were recorded prebleach, postbleach, and postbleach plus 30 s. Exo84-YFP fluorescence was quantified as the fractional area of the tip above background fluorescence intensity. Recovery was defined as $(I_{30} - I_b)/(I_0 - I_b) \times 100\%$, where I_0, I_b, and I_{30} are the values of Exo84-YFP fluorescence prebleach, postbleach, and 30-s postbleach, respectively. ns, nonsignificant ($p > 0.05$).

Exocyst complex coimmunoprecipitation

Cells were broken in IP-Lysis buffer (5% glycerol, 50 mM Tris-HCl, pH 7.5, 150 mM KCl, 2 mM $MgCl_2$, 0.5 mN ethylene glycol tetraacetic acid, 1 mM DTT, and protease inhibitor tablet [Roche]). Immunoprecipitation was done as described, using anti-GFP or anti-HA antibodies.

In vitro kinase assays

Cdc28-HA or Cdc28as-HFP was immunoprecipitated in hyphal lysates using anti-HA (12CA5) monoclonal antibody. Kinase assays were carried out as previously described (Bishop *et al.*, 2010). The anti–pS-Cdk antibody was used to detect Cdk1-specific phosphorylation.

Phospholipid-binding assay

Recombinant glutathione *S*-transferase (GST)–Exo84, GST-Exo84-3A, and GST-Exo84-3E were expressed in *E. coli* and purified with glutathione Sepharose 4b (GE Healthcare) according to the manufacturer's instructions. For the strips shown in Figure 9C, 8 µg of purified GST-Exo84-3E and 2 µg of purified GST-Exo84 protein were incubated with a PIP Strip (Echelon Biosciences, Salt Lake City, UT) previously blocked with 3% bovine serum albumin. Protein binding was visualized using anti-GST antibody (Santa Cruz Biotechnology, Dallas, TX).

Microscopy

Live-cell imaging was carried out on cells growing on agar pads using a DeltaVision RT microscope (Applied Precision Instruments, Seattle, WA) as described previously (Bishop *et al.*, 2010). The intensity of the Mlc1-YFP signal in the Spitzenkörper shown in Figure 2 was measured using the plot *Z*-axis profile tool in the FIJI distribution of ImageJ (http://fiji.sc/Fiji) after a region of interest (ROI) had been drawn around the area occupied by the Spitzenkörper in frames 43–58 of Supplemental Movie S2. The data are shown with the background measured within the cell subtracted. The images shown in Figure 5 were obtained from cells grown in YEPD liquid culture 120 min after hyphal induction and stained in phosphate-buffered saline (PBS) buffer with Calcofluor white (Fluorescent Brightener 28; Sigma-Aldrich) at a concentration of 1 µg/ml. To quantify cell dimensions and morphology shown in Figure 5, hyphal cells were grown for 120 min in YEPD liquid culture as described. After harvesting, the cells were fixed with 2% formaldehyde and then treated with pepsin to dissociate clumped hyphae as previously described (Sudbery, 2001). Cell dimensions were measured using FIJI aided by an in-house custom script that recorded cell dimensions and user-defined definitions of morphological state (hyphae, pseudohyphae, or other). Calcofluor white (Fluorescent Brightener 28) was added to liquid grown cells at a concentration of 1 µg/ml. FRAP experiments were carried out using a DeltaVision Microscope with an attached 532-nm laser module for bleaching. Images were analyzed in FIJI as follows. For each image a threshold was set to exclude the background. An ROI was drawn around the crescent of Exo84 in the prebleach image. The fractional area above the threshold in prebleach, postbleach, and postbleach plus 30-s images was then recorded. Recovery was defined as $(I_{30} - I_b)/(I_0 - I_b) \times 100\%$, where I_0, I_b, and I_{30} are the values of Exo84-YFP intensity prebleach, postbleach, and 30-s postbleach, respectively

Protein threading

The Protein Homology/Analogy Recognition Engine, version 2.0 (Phyre2), in its intensive modeling mode was use to obtain the Exo84 structure (Kelley and Sternberg, 2009). Analysis, formatted, and final movies and images were created using PyMOL (PyMOL Molecular Graphics System, version 1.2r3pre; Schrödinger).

ACKNOWLEDGMENTS

We thank Jeremy Craven and Sam Barnett for custom scripts to run within the FIJI version of ImageJ that was used in the quantitation of the micrographs. We thank the Berman, Wang, and Wendland laboratories for strains and plasmids. This work was supported by Biotechnology and Biological Sciences Research Council Project Grant BB/J002305/1.

REFERENCES

Adamo JE, Rossi G, Brennwald P (1999). The Rho GTPase Rho3 has a direct role in exocytosis that is distinct from its role in actin polarity. Mol Biol Cell 10, 4121–4133.

Bensen ES, Clemente-Blanco A, Finley KR, Correa-Bordes J, Berman J (2005). The mitotic cyclins Clb2p and Clb4p affect morphogenesis in *Candida albicans*. Mol Biol Cell 16, 3387–3400.

Bishop A, Lane R, Beniston R, Lazo B, Smythe C, Sudbery P (2010). Hyphal growth in *Candida albicans* requires the phosphorylation of Sec2 by the Cdc28-Ccn1/Hgc1 kinase. EMBO J 29, 2930–2942.

Boyd C, Hughes T, Pypaert M, Novick P (2004). Vesicles carry most exocyst subunits to exocytic sites marked by the remaining two subunits, Sec3p and Exo70p. J Cell Biol 167, 889–901.

Brennwald P, Rossi G (2007). Spatial regulation of exocytosis and cell polarity: yeast as a model for animal cells. FEBS Lett 581, 2119–2124.

Caballero-Lima D, Kaneva IN, Watton SP, Sudbery PE, Craven CJ (2013). The spatial distribution of the exocyst and actin cortical patches is sufficient to organize hyphal tip growth. Eukaryot Cell 12, 998–1008.

Chapa-Y-Lazo B, Lee S, Regan H, Sudbery P (2011). The mating projections of *Saccharomyces cerevisiae* and *Candida albicans* show key characteristics of hyphal growth. Fungal Biol 115, 547–556.

Chen YL, Montedonico AE, Kauffman S, Dunlap JR, Menn FM, Reynolds TB (2010). Phosphatidylserine synthase and phosphatidylserine decarboxylase are essential for cell wall integrity and virulence in *Candida albicans*. Mol Microbiol 75, 1112–1132.

Court H, Sudbery P (2007). Regulation of Cdc42 GTPase activity in the formation of hyphae in *Candida albicans*. Mol Biol Cell 18, 265–281.

Crampin H, Finley K, Gerami-Nejad M, Court H, Gale C, Berman J, Sudbery PE (2005). *Candida albicans* hyphae have a Spitzenkorper that is distinct

from the polarisome found in yeast and pseudohyphae. J Cell Sci 118, 2935–2947.
Finger FP, Hughes TE, Novick P (1998). Sec3p is a spatial landmark for polarized secretion in budding yeast. Cell 92, 559–571.
Gola S, Martin R, Walther A, Dunkler A, Wendland J (2003). New modules for PCR-based gene targeting in *Candida albicans*: rapid and efficient gene targeting using 100 bp of flanking homology region. Yeast 20, 1339–1347.
Goranov AI, Amon A (2010). Growth and division not a one-way road. Curr Opin Cell Biol 22, 795–800.
Guo W, Tamanoi F, Novick P (2001). Spatial regulation of the exocyst complex by Rho1 GTPase. Nat Cell Biol 3, 353–360.
He B, Guo W (2009). The exocyst complex in polarized exocytosis. Curr Opin Cell Biol 21, 537–542.
He B, Xi F, Zhang X, Zhang J, Guo W (2007a). Exo70 interacts with phospholipids and mediates the targeting of the exocyst to the plasma membrane. EMBO J 26, 4053–4065.
He B, Xi FG, Zhang J, TerBush D, Zhang XY, Guo W (2007b). Exo70p mediates the secretion of specific exocytic vesicles at early stages of the cell cycle for polarized cell growth. J Cell Biol 176, 771–777.
Heider MR, Munson M (2012). Exorcising the exocyst complex. Traffic 13, 898–907.
Jones LA, Sudbery PE (2010). Spitzenkorper, exocyst and polarisome components in *Candida albicans* hyphae show different patterns of localization and have distinct dynamic properties. Eukaryot Cell 9, 1455–1465.
Kelley LA, Sternberg MJ (2009). Protein structure prediction on the Web: a case study using the Phyre server. Nat Protocols 4, 363–371.
Klis FM, Boorsma A, De Groot PWJ (2006). Cell wall construction in *Saccharomyces cerevisiae*. Yeast 23, 185–202.
Lavoie H, Sellam A, Askew C, Nantel A, Whiteway M (2008). A toolbox for epitope-tagging and genome-wide location analysis in *Candida albicans*. BMC Genomics 9, 578–591.
Lee KL, Buckley HR, Cambell CC (1975). An amino acid liquid synthetic medium for the development of mycelial and yeast forms of *Candida albicans*. Sabouraudia 13, 148–153.
Li CR, Lee RT-H, Wang YM, Zheng XD, Wang Y (2007). *Candida albicans* hyphal morphogenesis occurs in Sec3p-independent and Sec3p-dependent phases separated by septin ring formation. J Cell Sci 120, 1898–1907.
Luo G, Zhang J, Luca FC, Guo W (2013). Mitotic phosphorylation of Exo84 disrupts exocyst assembly and arrests cell growth. J Cell Biol 202, 97–111.
McCusker D, Denison C, Anderson S, Egelhofer TA, Yates JR, Gygi SP, Kellogg DR (2007). Cdk1 coordinates cell-surface growth with the cell cycle. Nat Cell Biol 9, 506-U45.
Punta M *et al*. (2012). The Pfam protein families database. Nucleic Acids Res 40, D290–D301.
Roumanie O, Wu H, Molk JN, Rossi G, Bloom K, Brennwald P (2005). Rho GTPase regulation of exocytosis in yeast is independent of GTP hydrolysis and polarization of the exocyst complex. J Cell Biol 170, 583–594.
Sandquist JC, Kita AM, Bement WM (2011). The dead shall rise: actin and myosin return to the spindle. Dev Cell 21, 410–419.
Schaub Y, Dunkler A, Walther A, Wendland J (2006). New pFA-cassettes for PCR-based gene manipulation in *Candida albicans*. J Basic Microbiol 46, 416–429.
Sinha I, Wang YM, Philp R, Li CR, Yap WH, Wang Y (2007). Cyclin-dependent kinases control septin phosphorylation in *Candida albicans* hyphal development. Dev Cell 13, 421–432.
Siniossoglou S, Pelham HRB (2002). Vps51p links the VFT complex to the SNARE Tlg1p. J Biol Chem 277, 48318–48324.
Soll DR, Herman MA, Staebell MA (1985). The involvement of cell wall expansion in the two modes of mycelium formation of *Candida albicans*. J Gen Microbiol 131, 2367–2375.
Sudbery PE (2001). The germ tubes of *Candida albicans* hyphae and pseudohyphae show different patterns of septin ring localisation. Mol Microbiol 41, 19–31.
Sudbery PE (2011). Growth of *Candida albicans* hyphae. Nat Rev Microbiol 9, 737–748.
Sudbery PE, Gow NAR, Berman J (2004). The distinct morphogenic states of *Candida albicans*. Trends Microbiol 12, 317–324.
Terbush DR, Maurice T, Roth D, Novick P (1996). The exocyst is a multiprotein complex required for exocytosis in *Saccharomyces cerevisiae*. EMBO J 15, 6483–6494.
Terbush DR, Novick P (1995). Sec6, Sec8, and Sec15 are components of a multisubunit complex which localizes to small bud tips in *Saccharomyces cerevisiae*. J Cell Biol 130, 299–312.
Walther A, Wendland J (2008). Hyphal growth and virulence in *Candida albicans*. In: Human and Animal Relationships, ed. AA Brakhage and PF Zipfel, Berlin: Springer-Verlag, 95–114.
Wang A, Raniga PP, Lane S, Lu Y, Liu HP (2009). Hyphal chain formation in *Candida albicans*: Cdc28-Hgc1 phosphorylation of Efg1 represses cell separation genes. Mol Cell Biol 29, 4406–4416.
Wightman R, Bates S, Amnorrattapan P, Sudbery PE (2004). In *Candida albicans*, the Nim1 kinases Gin4 and Hsl1 negatively regulate pseudohypha formation and Gin4 also controls septin organization. J Cell Biol 164, 581–591.
Wilson B, Davis D, Mitchell AP (1999). Rapid hypothesis testing in *Candida albicans* through gene disruption with short homology regions. J Bacteriol 181, 1868–1874.
Wu H, Turner C, Gardner J, Temple B, Brennwald P (2010). The Exo70 subunit of the exocyst is an effector for both Cdc42 and Rho3 function in polarized exocytosis. Mol Biol Cell 21, 430–442.
Zhang XY, Bi EF, Novick P, Du LL, Kozminski KG, Lipschutz JH, Guo W (2001). Cdc42 interacts with the exocyst and regulates polarized secretion. J Biol Chem 276, 46745–46750.
Zhang X, Orlando K, He B, Xi F, Zhang J, Zajac A, Guo W (2008). Membrane association and functional regulation of Sec3 by phospholipids and Cdc42. J Cell Biol 180, 145–158.
Zheng XD, Lee RTH, Wang YM, Lin QS, Wang Y (2007). Phosphorylation of Rga2, a Cdc42 GAP, by CDK/Hgc1 is crucial for *Candida albicans* hyphal growth. EMBO J 26, 3760–3769.
Zheng X, Wang Y, Wang Y (2004). Hgc1, a novel hypha-specific G1 cyclin-related protein regulates *Candida albicans* hyphal morphogenesis. EMBO J 23, 1845–1856.